Minijet scale and energy loss at relativistic energies in event generator models

V. Topor Pop,[1] M. Gyulassy,[2] J. Barrette,[1] C. Gale,[1] X. N. Wang,[3] N. Xu,[3] and K. Filimonov[3]

[1]*McGill University, Montreal, Canada H3A 2T8*
[2]*Physics Department, Columbia University, New York, New York, 10027, USA*
[3]*Nuclear Science Division, LBNL, Berkeley, California, 94720, USA*

Recent data from relativistic heavy ion collider on rapidity and transverse momentum distributions of hadrons produced in ultrarelativistic reaction of both Au+Au and $p+p$ are compared to predictions of the HIJING and RQMD models. The original default minijet scale $p_0=2$ GeV/c and energy loss, dE/dx $=2$ GeV/fm in HIJING lead to a too rapid growth of the multiplicity with energy. RQMD model without minijet leads on the other hand to a too slowly increasing multiplicity with energy. Therefore, we study what variations of p_0 and dE/dx are required in HIJING to account for the observed N_{part} and $\sqrt{s}$ dependence of the global dN_{ch}/dy and dE_T/dy observables as well as the jet quenching pattern out to $p_T \sim 8$ GeV. We show that a slight increase of p_0 from the default 2.0 GeV/c at $\sqrt{s}=130A$ GeV to 2.2 GeV/c at $\sqrt{s}=200A$ GeV is sufficient to account for the bulk observables. Jet quenching of π^0 above $p_T>4$ GeV/c at $200A$ GeV is found to be well reproduced in central $Au+Au$ by the original HIJING default prediction. However, the effective surface emission in the HIJING model formulation of energy loss overpredicts the quenching in more peripheral collisions. Neither HIJING nor HIJING/$B\bar{B}$ can account for the observed anomalous excess of moderate $p_T<4$ GeV/c baryons. The agreement of RQMD with data in this p_T region is shown to be fortuitous because, without minijets, it fails to reproduce the $p+p$ spectrum.

I. INTRODUCTION

Qualitatively new phenomena have been discovered [1,2] in ultrarelativistic nuclear collisions at total center of mass energy $E_{c.m.}=(130–200)A$ GeV at the relativistic heavy ion collider (RHIC) and interpreted as evidence for the formation of ultradense QCD matter. The extensive systematics of both bulk global observables and high transverse momentum phenomena were reported by PHENIX [3–13], STAR [14–23], PHOBOS [24–31], and BRAHMS [32–36]. RHIC data are now available not only for Au+Au collisions but also for $p+p$ with high statistics, to accurately calibrate the magnitude of nuclear effects, and also $d+$Au [13,23,31,36] needed as a control experiment to separate initial versus final state interaction effects.

In this paper we compare predictions of the HIJING [37] and RQMD [38] models to data. These nuclear collision event generators were developed a decade ago and continue to be useful tools for detector design and interpretation of experimental results because they simulate complete exclusive event characteristics at SPS and RHIC. HIJING, incorporating pQCD minijet production, is constrained to reproduce essential features of $p+p$ data over a wide energy range. RQMD is designed to simulate only soft multiparticle production at lower energies, but is of interest since it incorporates a model of final state interaction. No attempt is made here to review the many other models developed since the release of HIJING and RQMD. We refer the reader to Refs. [39–76] for a broader perspective.

Our goal is to test specific predictions within HIJING and RQMD models, made well in advance of the data. The predictions involved estimating key physical parameters controlling the dynamics. An important aim of this paper is to investigate what adjustments of those parameters may be required in light of the new data. The two main parameters of HIJING that we concentrate on in this paper are (1) the separation scale p_0 between the perturbative (pQCD) minijet processes and the phenomenological soft (beam jet fragmentation) processes and (2) the energy loss dE/dx of high transverse momentum partons propagating through the dense (quark-gluon plasma) medium produced in the reaction.

The minijet separation scale, $p_0 \approx 2$ GeV/c, assumed in HIJING [37] controls the $\sqrt{s}$ dependence of the bulk multiplicity and transverse energy observables as well as their centrality dependence on the number of wounded nucleon participants, N_{part}. RQMD [38] and its UrQMD [39,71] extensions assume in effect that $p_0 \rightarrow \infty$ and therefore neglect the power law tails due to pQCD minijets. The default constant value of $p_0=2$ GeV/c in HIJING was fixed by fitting pp data through Tevatron energies [37], and it was assumed to be *independent* of both $\sqrt{s}$ and A in order to predict multiparticle observables in AA that extrapolate down accurately to $A=1$ to reproduce experimentally known pp data. In RQMD, there was no attempt to fit collider energy pp data. Our approach differs in this major respect from many recent models that fail to account for multiparticle phenomena in $p+p$ collisions. Our philosophy is that due to the myriad of dynamical complexities already displayed in "elementary" $p+p$ reactions, any model proposed to explain $A+A$ collisions must extrapolate accurately down to $A=1$. This is because one of the very few experimental knobs in heavy ion reactions is the variation of the impact parameter through the participant number dependence of observables. In peripheral collisions the observables necessarily approach their value in $p+p$ collisions.

Recently, several models were developed that challenge the assumption that the separation scale p_0 is independent of both $\sqrt{s}$ and A as in HIJING, Refs. [57,58] generalized the minijet scale by allowing it to vary dynamically by introducing the hypothesis of *final state saturation* (FSS) of the produced minijet density per unit area. That saturation scale was predicted to be $p_s(s,A)=1.1$ GeV$(\sqrt{s}/200)^{0.128}(A/200)^{0.191}$. This hypothesis leads to a specific prediction for the initial parton distribution in $A+B$ collisions. With the additional hypothesis that this initial condition evolves according to local thermal hydrodynamics, the p_T integrated global observables in central Au+Au were shown to be well accounted for. However, the breakdown of hydrodynamics and the smallness of p_s($p_s < 1$ GeV/c) in peripheral collisions prevents the model from predicting correctly peripheral $A+A$ collisions and $p+p$ collisions.

An alternate *initial state saturation* (ISS) hypothesis for the variation of the separation scale was introduced in Refs. [59–63,77,78]. In this picture, p_0 is replaced by a gluon saturation scale $Q_s(s,A) \approx 1.4$ GeV$(\sqrt{s}/200)^{0.3}(A/200)^{1/6}$. This saturation scale is considered to be the boundary of the classical Yang-Mills field domain. Instead of hydrodynamics, local parton hadron duality is assumed to predict low $p_T \sim Q_s$ integrated bulk global observables. The normalization of Q_s was fixed by fitting the observed central 130A GeV Au+Au rapidity density. ISS was found to be more successful in describing the lower participant number and $\sqrt{s}$ dependence of the rapidity density at RHIC than the FSS model due to a particular low $Q^2 \sim 1$–2 GeV^2 dependence of the gluon structure function and fine structure coupling. While preliminary extensions [62] of this ISS model to the $p_T > Q_s$ regime could fit central 130A GeV Au+Au without final state interactions, the most recent data on d+Au reactions [13,23,31,36] rule out a particular extension [63] of the ISS model at mid rapidity in the range $2 < p_T < 10$ GeV/c.

While neither ISS or FSS saturation models can describe simultaneously the global low-p_T and the hard high-p_T observables in both $p+p$ and $A+A$ collisions, they both provide strong motivation to test the effects of variations of p_0 with both s and A in HIJING. With this motivation, the first part of this paper will be to investigate, within the HIJING model, the effect of relaxing the (s,A) independence of the default constant $p_0=2$ GeV/c assumption. Importantly, we seek to do this while retaining our philosophy that critical features of multiparticle production in $p+p$ should be accounted for simultaneously in the same model. Our first conclusion will be that the global 130–200A GeV Au+Au data can be well accounted for by allowing a rather modest 10% (A-independent) enhancement of p_0 from 2 GeV/c at 130A GeV to about 2.2 GeV/c at 200A GeV.

The second part of this paper focuses on jet quenching [79]. Jet quenching is one of the most striking new phenomena [6,11,17,20,22,30] discovered at RHIC. This effect was not observed previously at lower energies. In fact, at SPS a strong (Cronin) enhancement of high p_T π^0 was observed [80].

The first quantitative predictions of jet quenching with HIJING [37,81] assumed a default constant dE/dx $=2(1)$GeV/fm gluon (quark) energy loss and was implemented by a simple string flip algorithm assuming a mean free path of $\lambda=1$ fm. As recently reviewed in Refs. [40,82], there has been considerable progress since that time in computing the dependence of medium induced radiative energy loss, $\Delta E(p_T,L,\rho_0)$, in QCD [45–47,52,53,82]. The observable consequences of the dependence of ΔE on the jet energy, its propagation length, and the evolving parton density have been explored in pQCD models in which the plasma is assumed rather than calculated dynamically. While the jet quenching algorithm in HIJING is much more schematic, the model provides a useful theoretical laboratory to study its observable consequences in the dynamical medium that it creates. In the second part of this paper, we therefore explore what modifications of the default HIJING assumptions are required in light of the new data.

As we show below, the default constant energy loss in HIJING accounts remarkably well for the high-$p_T\pi^0$ suppression pattern in central Au+Au at 200A GeV. In fact, HIJING also accounts [83] for the enhancement observed [80] at SPS that is otherwise puzzling according to pQCD estimates [84]. However, we show below that HIJING fails to account for the observed centrality dependence as well as for the anomalous baryon enhancement observed up to 5 GeV. HIJING/B [85–87], with its implementation of baryon junctions [88,89], was tested to see if this mechanism could account for the baryon anomaly (see also Ref. [48]). However, the present version (HIJING/BBv1.10) fails to account for the large transverse slopes of antibaryons and does not reproduce the "baryon lump" at moderate p_T in the nuclear modification factor.

While RQMD [38] does not contain minijets, we investigate its predictions because it is one of the first models to simulate final state transport dynamics of prehadrons and hadrons without assuming local equilibrium as in hydrodynamics. It was able to reproduce the directed and elliptic collective flow systematics observed in Pb+Pb at SPS (17A GeV). However, as we show below, the absence of hard pQCD processes leads to a much too weak beam energy dependence at RHIC energies. It therefore also fails to account for the power law tails of the $p+p$ spectra at 200 GeV. We refer to Refs. [71,72] for a review of application of RQMD and UrQMD applied to reactions at AGS and SPS energies.

While not addressed directly in this paper, we call attention to the recent AMPT transport model [65] that incorporates minijet production and extends HIJING by including both parton cascading and hadronic final state interactions. AMPT is under extensive development and has been tested on a number of important RHIC observables [65–68]. However, problems with covariance of numerical solutions involving ultrarelativistic parton cascading [69,70] require very high parton subdivision techniques which are unfortunately beyond present computer power to solve with AMPT.

In order to bypass current technical difficulties of predicting bulk collective phenomena via transport theory, hydrodynamic models have also been extensively applied [41,90–97]. The central simplifying dynamical assumption is that perfect local equilibrium is established and maintained
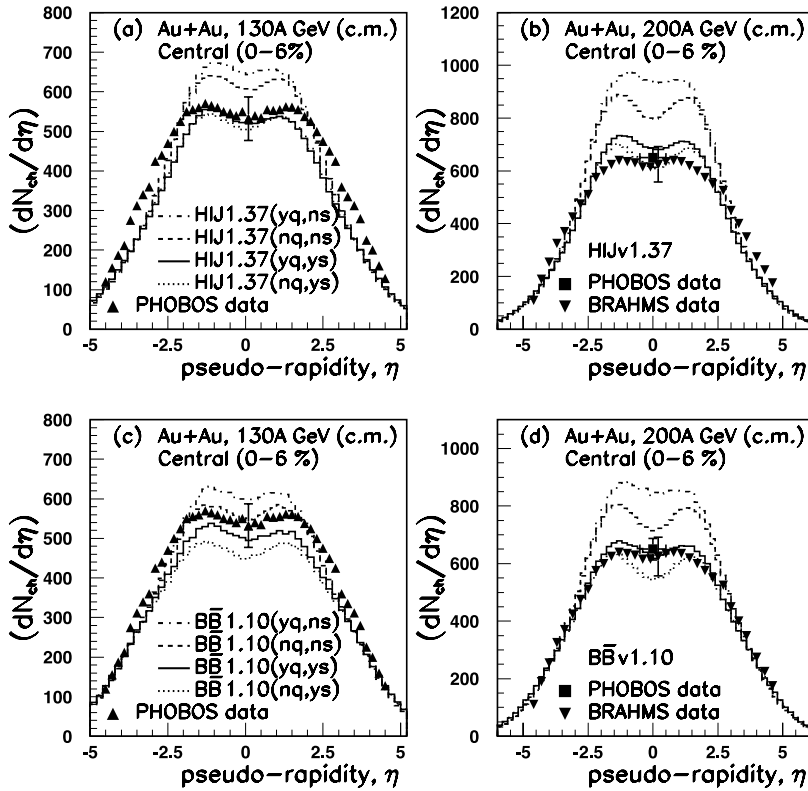
FIG. 1. Charged hadron rapidity distributions for central (0–6%) Au+Au collisions as function of c.m. energies. The histograms show the theoretical predictions from HIJING v1.37 (upper part) and HIJING/B$\bar{\text{B}}$ v1.10 (lower part) with (y) or without (n) effects of quenching q or/and shadowing s included. The data are from PHOBOS Collaboration [26] (a), [27] (b), [28] (c), and BRAHMS Collaboration [33] (c). The error bars at midrapidity include systematic uncertainties. The other error bars of the order of 10–15% have been omitted for clarity.

throughout the reaction. Therefore nonviscous hydrodynamics together with a Cooper-Frye statistical freeze-out prescription [98] are used to compute the expansion, hadronization, and subsequent expansion until freeze-out. No attempt is made in such models to compute the initial condition, but rather the initial entropy and baryon density are fit to the measured rapidity distributions. While such models cannot predict beam energy dependence of observables, they do predict striking collective flow phenomena and their dependence on the QCD equation of state (for a recent review of hydrodynamics at RHIC see Ref. [41]). The first attempt at a hybrid combination hydrodynamics and jet quenching was proposed in Ref. [49]. Recently, an important step forward is the development of a consistent 3+1D (where 1D stands for one-dimensional) hydrodynamical approach including QCD jet quenching [97].

Unlike hydrodynamics [41,97] or parton transport models [66,69], neither HIJING nor RQMD can predict the large amplitude elliptic flow observed [15,21,7,29] at RHIC. Elliptic flow is especially sensitive to early partonic final state interactions beyond the capability of these models. However, azimuthally integrated inclusive spectra are still interesting and can be addressed by models considered here. We use the following versions of HIJING v1.37 [37], HIJING/B$\bar{\text{B}}$ v1.10 [85,86], and RQMD v2.4 [38] for the computations reported below.

II. CHARGED PARTICLE DISTRIBUTIONS AND THE MINIJET SCALE

Recent measurements of the rapidity density of charged particles in Au+Au collisions over the range of total nucleon-nucleon center of mass (c.m.) energy $\sqrt{s_{NN}}$ =56–200 GeV, have been reported [4–6,8,16,17,26–28,33]. Within the errors, an approximatively logarithmic rise of charged particle rapidity density *per participating baryon pair* ($dN_{ch}/d\eta/0.5N_{part}$) with $\sqrt{s_{NN}}$ is observed over the full range of collision energies [28]. In Refs. [99,100] the centrality dependence of this observable was proposed as a test of the nuclear enhancement of the minijet component as well as whether gluon saturation is reached at RHIC energies. The predictions of different models varied prior to the data greatly in the range $dN_{ch}/dy \sim 700$–1500 at mid-rapidity for Au+Au central collisions [39].

The predictions of HIJING [Figs. 1(a) and 1(b)] and HIJING/B$\bar{\text{B}}$ [Figs. 1(c) and 1(d)] with (y) or without n effects of quenching q or/and shadowing s are presented in Fig. 1. The data from PHOBOS [26–28] and BRAHMS [33] experiments at $\sqrt{s_{NN}}$=130 GeV and $\sqrt{s_{NN}}$=200 GeV are shown for comparison. In all cases, both quenching and possible parton shadowing influence the predicted pseudorapidity distribution $dN_{ch}/d\eta$ in this energy range. However, these effects work in opposite direction and thus partially cancel each other. Without shadowing as assumed in the default HIJING model, the flux of minijets with $p_T > 2$ GeV/c is too high and $dN_{ch}/d\eta$ is overestimated. Even with the larger shadowing at the smaller x at $\sqrt{s_{NN}}$=200 GeV, the gluon density enhancement resulting from minijet energy loss leads to a 10–20% overestimate of the charged particle rapidity density in going from 130A to 200A GeV in Fig. 1(b). A similar tendency is seen in the B$\bar{\text{B}}$ version of HIJING which, however, better accounts for the width of the rapidity distributions. The width is sensitive to the nuclear fragmentation
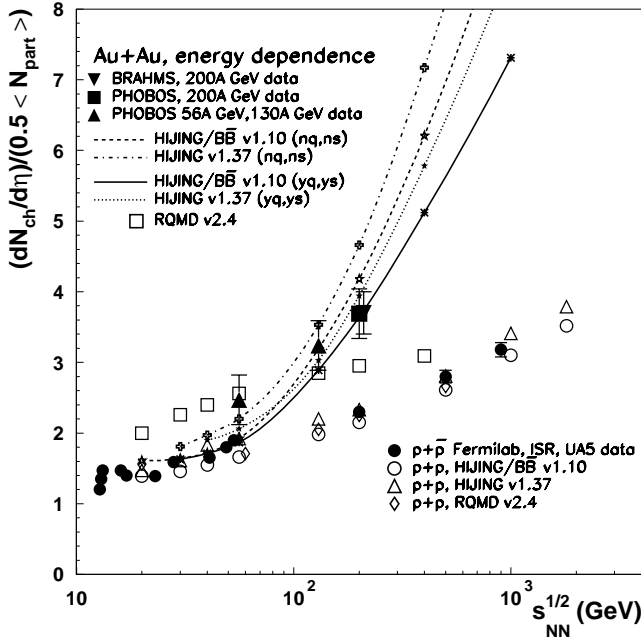
FIG. 2. Charged particle rapidity density *per participating baryon pair* versus the c.m. energy. The predictions of HIJING/B$\bar{\text{B}}$ v1.10 (yq, ys)—full line, HIJING/B$\bar{\text{B}}$ v1.10 (nq, ns)—dashed line, HIJING v1.37 (yq, ys)—dotted line, HIJING v1.37 (nq, ns)—dot-dashed line, and RQMD v2.4 (*open squares*) are compared to data. The data for the central (0–6%) Au+Au collisions are from PHOBOS [26,28], and from BRAHMS [33]. The error bars include systematic uncertainties; pp and $p\bar{p}$ data are from Refs. [101–104]; the error bars are statistical only.

physics, especially baryon number transport from the beam rapidities. HIJING/B$\bar{\text{B}}$ can better account for nuclear fragmentation by introducing the greater baryon stopping power through the baryon junction mechanism.

These data are also consistent with the initial state saturation ISS model [33,59,60]. However, the EKRT final state saturation model [57] tends to overpredict the width of the rapidity distribution.

The energy dependence of the particle multiplicity is more easily seen in Fig. 2 where the central rapidity density per participant pair vs $\sqrt{s}$ of both HIJING and RQMD are compared to data. The PHOBOS data for the central (0–6%) Au+Au collisions are from Refs. [26–28]. The data for pp and $p\bar{p}$ are from Refs. [101–104]. Beginning about $\sqrt{s_{NN}}$ =100 GeV, the central Au+Au collisions show a significantly larger particle density per participant pair than in inelastic $p\bar{p}$ collisions. The energy dependence predicted by HIJING is strikingly different than that predicted by RQMD. While RQMD predicts a very small increase over the range $\sqrt{s_{NN}}$=56–200 GeV, HIJING predicts an increase of more than a factor of 1.3, which continues up to the highest energy calculated. This increase in HIJING is due to copious minijets production in $A+A$ collisions. RQMD fails to describe the trend of data because it misses the rise in multiplicity due to minijets. The predictions of both HIJING and HIJING/B$\bar{\text{B}}$ models are in better agreement with the data when the effects of both quenching and shadowing are included. Note that

with default energy loss $d\text{E}/dx$=2 GeV/fm and constant p_0 =2 GeV/c, the energy dependence obtained with HIJING is too rapid and the curves in Fig. 2 are for a reduced effective energy loss dE/dx=0.5 GeV/fm. One observes, however, that even this smaller energy loss still leads to a more rapid dependence on energy than seen in the data. The RQMD v2.4 curves were obtained using the *cascade mode* and taken into account its *rescattering* and *color rope* effects with their default parameters.

Another global probe of the dynamics is the transverse energy per charged particle, $dE_T/d\eta$ [4]. This distribution is sensitive to PdV work done by the plasma in hydrodynamical models. In HIJING its value depends again on the assumed shadowing and energy loss as seen in Fig. 3. In part (a) the total charged plus neutral transverse energy distribution is shown. In part (b) the contribution from only charged particle is shown. The results are for central (0–5%) Au +Au collisions at $\sqrt{s_{NN}}$=130 GeV. Both versions HIJING (yq, ys) and HIJING/B$\bar{\text{B}}$ seem to account better for the observed $dE_T/d\eta \approx$ 500 GeV than RQMD. This is again due to the absence of minijets in RQMD model.

We recall that FSS saturation model tend, in contrast, to overpredict [57] by a factor of 2–3 the transverse energy because the saturation scale $p_s \sim 1$ GeV/c is significantly smaller than the default p_0=2 GeV/c needed in HIJING to fit $p+p$ data. Therefore, FSS requires reduction of the initial transverse energy due to longitudinal hydrodynamic work. The same general tendency of overpredicting the transverse energy is found in classical Yang-Mills simulation of $A+A$ [43]. However, no detailed predictions of the transverse energy have been made within the KLN version [59–61] of ISS models.

Another important difference between the predictions of models is in the rapidity dependence of the transverse energy per particle [see Figs. 3(c) and 3(d)]. While RQMD predicts a relatively constant value between $-2.5 \leqslant \eta \leqslant 2.5$, both the numerator and denominator disagree with the data. HIJING gives on the other hand a rather strongly peaked distribution at midrapidity. This peaked distribution in HIJING is due to the localization of minijet production to central rapidities. Hydrodynamic models [41] generally assume a uniform boost invariant form of this ratio. We note that the PHOBOS observation [29] of a triangular dependence of the elliptic flow $v_2(y)$ peaked at midrapidity is very similar to the triangular pattern of $(dE_{Tall}/d\eta)/(dN_{ch}/d\eta)$ predicted by HIJING due to minijet production at 130A GeV. We are not aware of any predictions for this important global observable from saturation models. Figure 3(d) suggests that the initial conditions for hydrodynamics are not well approximated by Bjorken boost invariant forms [41] assumed thus far. A full 3+1D hydrodynamical simulation [97] with such more realistic boost variant initial conditions should be investigated to try to account for the PHOBOS elliptic flow.

The PHENIX data [4] show a value closer to 0.8 GeV for $(dE_{Tall}/d\eta)/(dN_{ch}/d\eta)$ that is remarkably independent of $\sqrt{s_{NN}}$ from 17 GeV to 130 GeV and also independent of centrality. The observed independence on energy and cen-
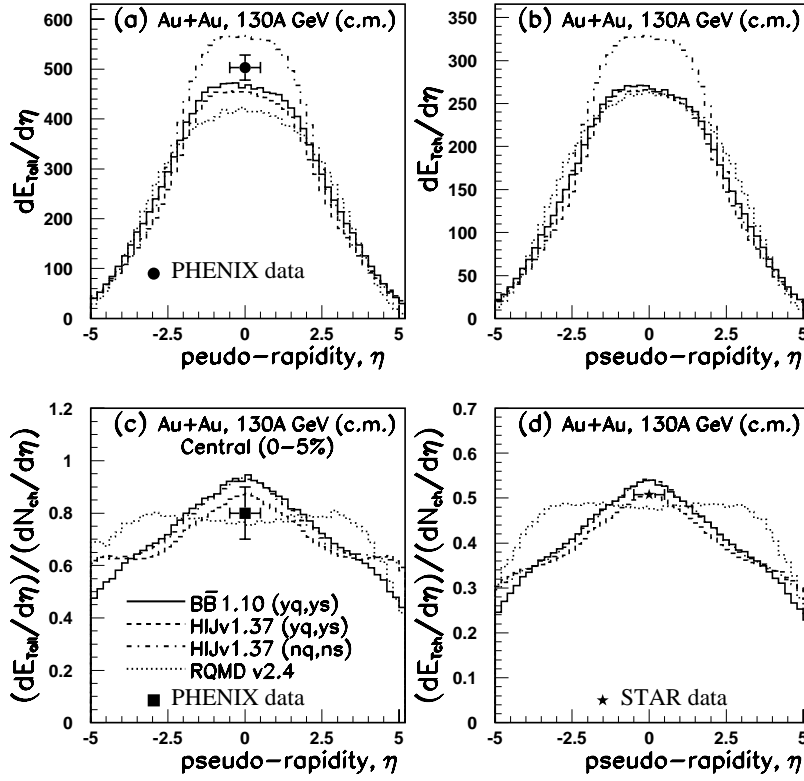
FIG. 3. Transverse energy distribution for (a) all particles, (b) charged particles only, (c) total transverse energy per charged particles, and (d) total transverse energy of charged particles per charged particles as a function of pseudorapidity. Theoretical predictions from HIJING/$\overline{BB}$ v1.10 (yq, ys)—solid, HIJING v1.37 (yq, ys)—dashed, HIJING v1.37 (nq, ns)—dash-dotted, and RQMD v2.4—dotted histograms are shown. The data are from PHENIX [5] and STAR [16]. The error bars for PHENIX include systematic uncertainties.

tralities is very interesting since it is difficult to obtain such an effect in any transport theory with pQCD relaxation rates [69,100].

We investigate next in more detail the centrality dependence of $dN_{ch}/d\eta$ (Fig. 4) and $dE_T/d\eta$ (Fig. 5) per pair of participating nucleons. Figures 4 and 5 show the results for

centrality dependence within HIJING v1.37 model calculations at $\sqrt{s_{NN}}=130$ GeV and $\sqrt{s_{NN}}=200$ GeV for (yq, ys) and (nq, ns) scenarios in comparison with experimental data [5,9,28,33]. The parameters employed for these calculations are shown in the figures. We note that all HIJING curves extrapolate at low multiplicities to the value $dN_{ch}/d\eta=2.2$,
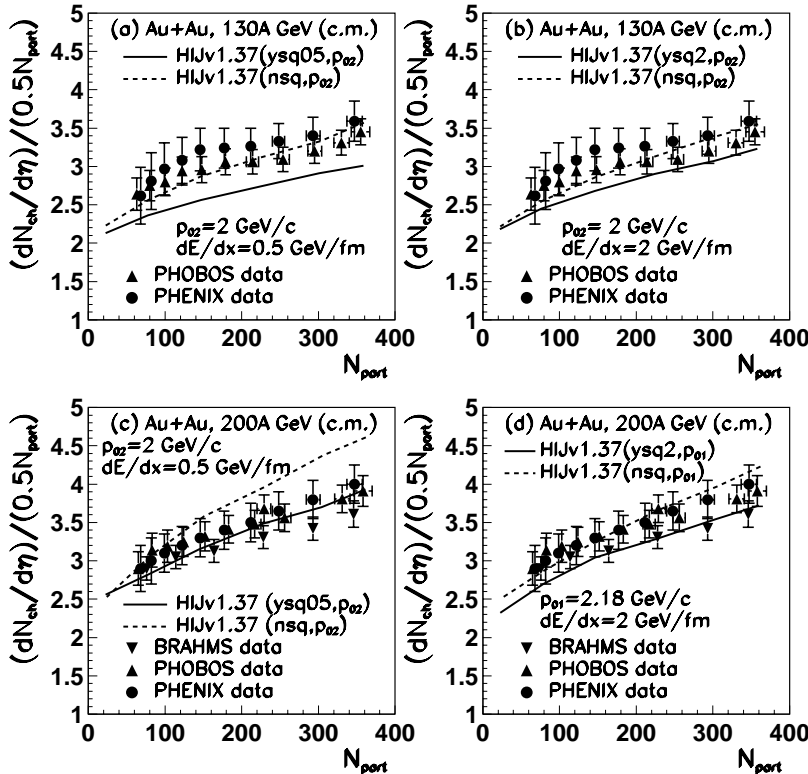

FIG. 4. Midrapidity $dN_{ch}/d\eta$ per participant pair as a function of the number of participants at $\sqrt{s_{NN}}=130$ GeV (upper part). Theoretical predictions from HIJING v1.37 model with (ysq—solid lines) and without (nqs—dashed lines) the effects of quenching and shadowing. The data at $\sqrt{s_{NN}}=130$ GeV are from PHENIX [5], Ref. [9], and PHOBOS [28]. Lower parts are the results at $\sqrt{s_{NN}}=200$ GeV. The data are from BRAHMS [33], PHOBOS [28], and PHENIX [9]. The parameters within HIJING calculations are given in the figure. The error bars include both statistical and systematic uncertainties.
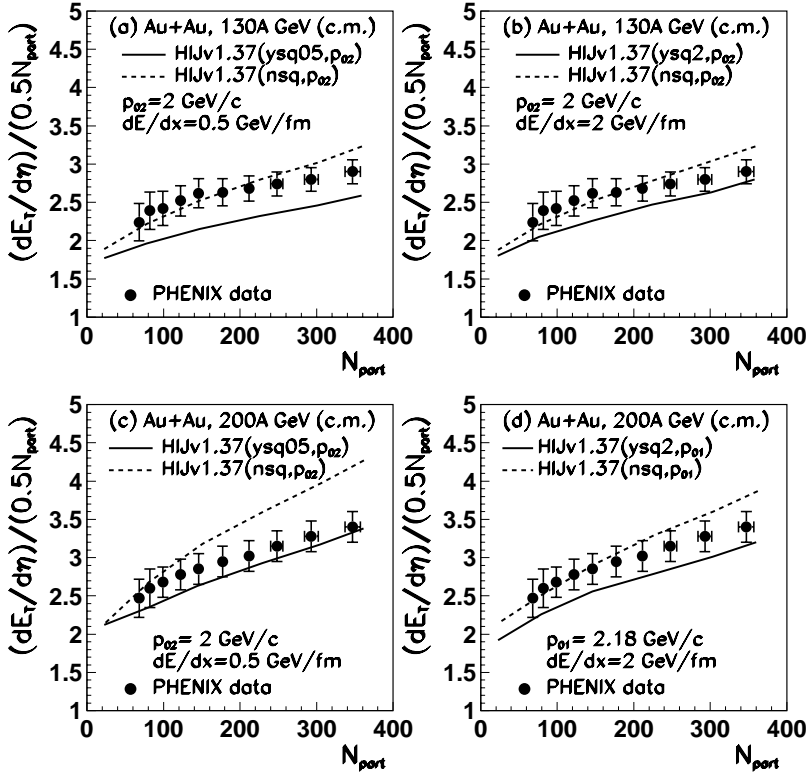
FIG. 5. Midrapidity $dE_T/d\eta$ *per participant pair* as a function of the number of participants at $\sqrt{s_{NN}}$=130 GeV (upper part) and $\sqrt{s_{NN}}$=200 GeV (lower part). Theoretical predictions from HIJING v1.37 model with (*ysq*—solid lines) and without (*nqs*—dashed lines) the effects of quenching and shadowing. The solid and dashed lines have the same meaning as in Fig. 4. The data at $\sqrt{s_{NN}}$=130 GeV are from PHENIX [5], Ref. [9], and PHOBOS [28], and at $\sqrt{s_{NN}}$=200 GeV the date are from BRAHMS [33], PHOBOS [28], and PHENIX [9]. The error bars include both statistical and systematic uncertainties.

observed in $p\bar{p}$ collisions by the UA5 Collaboration [101]. The HIJING model predicts steady rise in the particle production per participant pair although the data seem to have a slower variation with N_{part}. The predicted increase is due to nonlinear increase of hard scatterings, which in contrast to the beam jet fragments is dependent on the number of binary collisions. HIJING/BB̄ predicts a similar trend although the calculated values are lower than that given by HIJING by 10–15% and underpredicts the experimental results at $\sqrt{s_{NN}}$=130 GeV.

Figures 4(a) and 5(a) show the effect of lowering the energy loss to 0.5 GeV/fm as compared to a value of 2 GeV/fm used in Figs. 4(b) and 5(b). The default parameter predictions at $\sqrt{s_{NN}}$=130 GeV [Figs. 4(b) and 5(b)] are more consistent with data. However, for energy loss dE/dx =2.0 GeV/fm and p_0=2.0 GeV/c assumed to be independent of $\sqrt{s}$ it is found that the ratio of $R_{200/130}$ for midrapidity $dN_{ch}/d\eta$ is overpredicted for most central collisions by 30% as shown in Ref. [9]. This is a major failing of the HIJING assumption of energy independent minijet scale p_0 =2 GeV/c. Motivated by the energy dependence predicted by the saturation scales in FSS and ISS models discussed in the Introduction, and the data, we study in Figs. 4(d) and 5(d) the effect of allowing a slight increase with energy from $p_0(\sqrt{s})$=2.0 GeV/c at $\sqrt{s_{NN}}$=130 GeV to $p_0(\sqrt{s})$=2.18 GeV/c at $\sqrt{s_{NN}}$=200 GeV. Such an energy dependence was also found necessary in Ref. [54] using more modern structure functions than in HIJING.

Figure 6 (E_T/N_{ch} transverse energy per charged particle) and Fig. 7 (ratios $R_{200/130}$ for midrapidity $dN_{ch}/d\eta$ and $dE_T/d\eta$) present the results obtained within both models HIJING v1.37 (upper part) and HIJING/BB̄ v1.10 (lower

part). The data are much closer to the quench and shadowing (*yq, ys*) scenario.

It was shown [33] that hard scattering component to the charged particle production remains almost constant (36±6)% over the energy range $\sqrt{s_{NN}}$=130−200 GeV. We see when comparing the values from Figs. 4(d) and 5(d) to Figs. 4(c) and 5(c), and especially from Figs. 6 and 7, that the energy dependence of this global measure is reduced considerably to within the experiment range by allowing a modest increase of p_0 without assuming any additional N_{part} dependence of this scale. From these results we conclude that a 10% increase with energy of the minijet scale p_0 is required in both HIJING models to account for the centrality and energy dependence of the global multiplicity and transverse energy observables.

III. JET QUENCHING AND THE NUCLEAR MODIFICATION FACTOR

High-p_T hadron spectra, jet quenching, have been widely analyzed at SPS and RHIC energies [40]. We investigate in this section how well can HIJING and HIJING/BB̄ describe the high-p_T hadronic spectra in pp collisions and their predicted nuclear modifications in AA collisions.

The observation [11,13,17,20] of strong suppression of high-p_T hadron spectra in central Au+Au at RHIC energies [79,81,82] is the most dramatic new dynamical phenomenon discovered at RHIC relative to SPS. We recall that the comparison of parton model calculations and the experimental data does not show any evidence of parton energy loss at SPS energies [84]. The observed absence of quenching in d+Au [13,23,31,36], as predicted in Refs. [81,50,51,55,56],
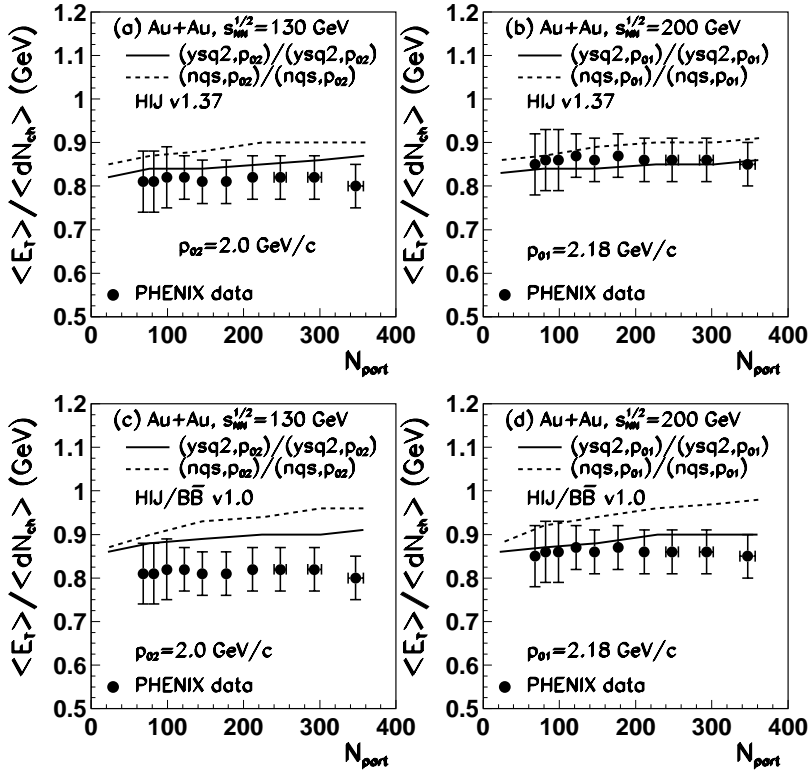
FIG. 6. Midrapidity ratios $(dE_T/d\eta)/dN_{ch}/d\eta$ as a function of the number of participants at $\sqrt{s_{NN}}$=130 GeV and $\sqrt{s_{NN}}$=200 GeV. Theoretical predictions within HIJING v1.37 (upper part) and HIJING/$\overline{BB}$ v1.10 (lower part) are shown. The solid and dashed lines have the same meaning as in Fig. 4. The data are from PHENIX [9]. The error bars include both statistical and systematic uncertainties.

proves that quenching is caused by final state interactions in the dense matter formed in Au+Au collisions and not due to gluon shadowing.

Parton-parton *hard scattering* with large momentum transfer produces high momentum quarks or gluons which fragment into jets of hadrons. The leading particles manifest themselves in a power-law like shape of the momentum distribution. High momentum partons are predicted to lose a significant fraction of their energy by gluon bremsstrahlung leading to a suppression of the high momentum tail of the single hadron inclusive spectra [81]. It has been argued that data from RHIC experiments show characteristic features
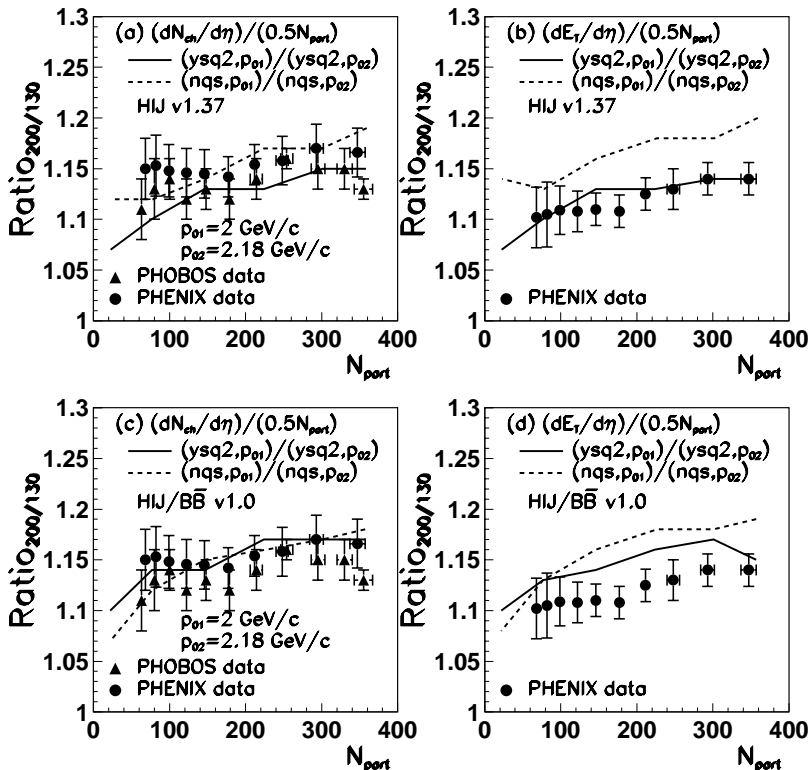

FIG. 7. Ratios $R_{200/130}$ for midrapidity $dN_{ch}/d\eta$ and $dE_T/d\eta$ *per participant pair* as a function of the number of participants. Theoretical predictions within HIJING v1.37 (upper part) and HIJING/$\overline{BB}$ v1.10 (lower part) model with (ysq, p_0) and without (nsq, p_0) the effects of quenching and shadowing are compared to the data [9]. For the labels of solid and dashed lines, see Figs. 4(b) and 4(d), and Figs. 5(b) and 5(d).
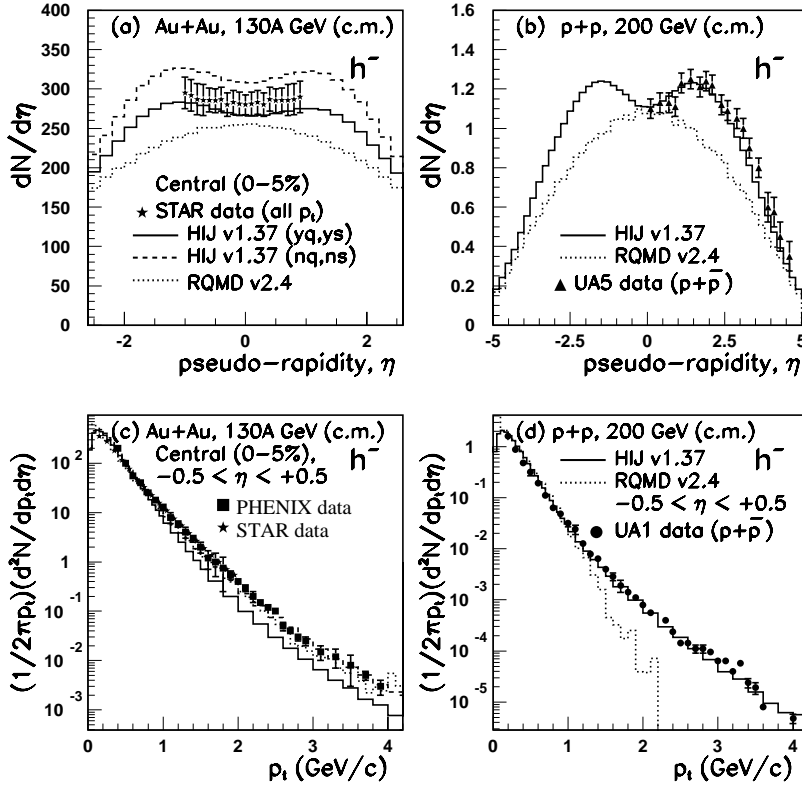
FIG. 8. Comparison of Au+Au and $p+p$ at RHIC energies is shown. (a) Negative hadrons pseudorapidity spectra for Au+Au collisions at $\sqrt{s_{NN}}$=130 GeV including STAR central (0–5%) data [16]. (b) $p+p$ at $\sqrt{s_{NN}}$=200 GeV including UA1 $p+\bar{p}$ data [101]. HIJING v1.37 (yq, ys)—solid, HIJING v1.37 (nq, ns)—dashed, and RQMD v2.4—dot-dashed histograms are theoretical calculations. Parts (c) and (d) compare the $p_\perp$ distributions. PHENIX data [6], STAR data [16], and UA1 data [104] are shown. The error bars include systematic uncertainties in part (a) and are statistical only in parts (b), (c), and (d).

consistent with such "*jet quenching effects*" [6,105,106]. Other interpretations have been proposed after the data became available. These are based on gluon saturation in the initial nuclear wave function [107], coherent fields and their geometry [108], surface emission of the quenched jets [109], final state hadronic interactions [110], and quark coalescence [111].

The default HIJING implementation of jet quenching uses a simplified algorithm most closely resembling surface emission. The energy loss is implemented by testing the number of interactions that a jet will have along its propagation line with excited participant *strings*. The approximate linear participant number scaling of the bulk multiplicity motivates this approximation to the transverse matter density profile through which the jets propagate. The distance between collisions is fixed by a mean free path parameter λ=1 fm by default. Energy loss is implemented by splitting the energy of the jet among multiple gluons with energies $\omega_i = \Delta z_i dE/dx$, where dE/dx=2(1) GeV/fm for gluon (quark) jets and Δz_i are distances between collisions. This simplified mechanism suppresses jets that originate more than one mean free path from the surface.

The effect of the nuclear modification is quantified in terms of the ratio [53]

$$R_{AA}(p_\perp) = \frac{d^2 N_{AA}/dy dp_\perp}{\langle N_{coll} \rangle d^2 N_{pp}/dy dp_\perp}, \qquad (1)$$

where $\langle N_{coll} \rangle$ is the average number of binary collisions of the event sample and can be calculated from the nuclear overlap integral T_{AA} and the inelastic nucleon-nucleon cross section: $\langle N_{coll} \rangle = \sigma_{nn}^{inel} \langle T_{AA} \rangle$. In the HIJING effective

surface emission model, we can expect $R_{AA} \propto (\lambda/N_{part}^{1/3} \text{ fm})$.

The absolutely normalized transverse momentum spectra and pseudo rapidity distributions for Au+Au central (0–5%) collisions [6,16] at $\sqrt{s_{NN}}$=130 GeV are shown in Fig. 8. We compare the STAR [16] pseudorapidity distribution of negative hadrons h^- for the central (0–5%) Au+Au collisions with the predictions from HIJING (yq, ys)—solid line, HIJING (nq, ns)—dashed line, and RQMD—dash-dotted line. The negative hadron pseudorapidity distributions in part (a) are best reproduced with shadowing and quenching effects present. Note in Fig. 8(c), however, that the moderate $1 < p_T < 4$ GeV spectra are too strongly overquenched by the default HIJING parameters. The "no shadow, no quench" calculation overpredicts the global rapidity density but remarkably fits the moderate p_T spectrum rather well. So where is the energy loss? As we discuss below, it is likely camouflaged by anomalous baryon excess.

Note that RQMD fits the moderate p_T h^- data better than HIJING (yq, ys). However, as shown in Fig. 8(b), the absence of minijet production in RQMD causes it to miss the observed features of the pp rapidity density [101] at $\sqrt{s_{NN}}$ =200 GeV that HIJING reproduces. Similarly, because of multiple jet production, HIJING reproduces the power-law-like tail of the $p+p$ p_T spectra very well while RQMD shows a glaring discrepancy [Fig. 8(d)]. This result is significant because it demonstrates that the agreement of RQMD in Fig. 8(c) is fortuitously due to a strong nuclear dependent Cronin-like multiple collision algorithm enhancement. This is similar to the fortuitous agreement [83] of HIJING with WA98 moderate p_T pion data at the SPS, where the results were shown to be exponentially sensitive to the Cronin algorithm adopted.
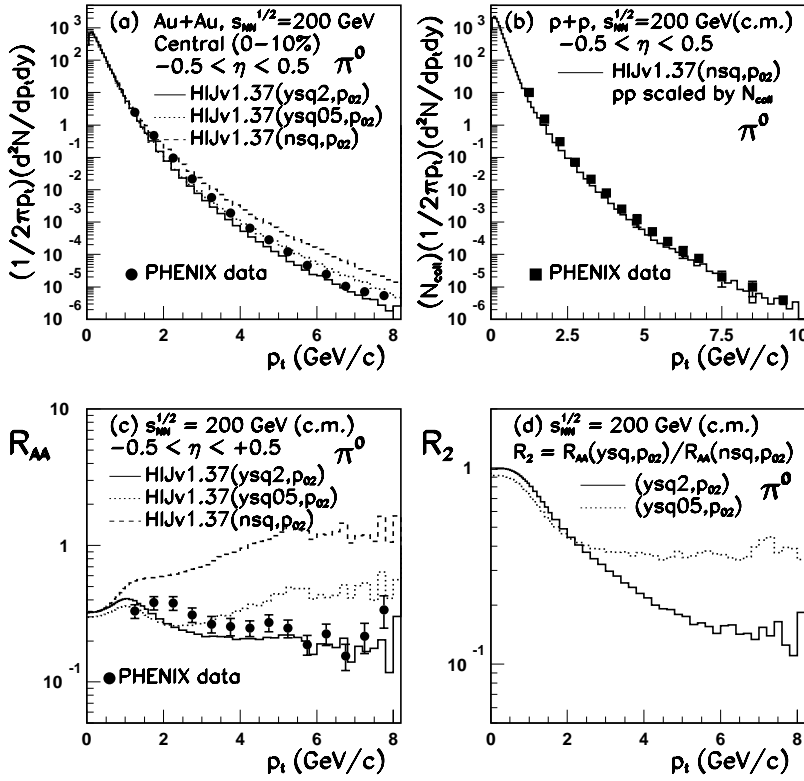
FIG. 9. Invariant yields at midrapidity for π^0 in central (0–10%) Au+Au collisions [part (a)] and scaled by number of binary collisions (N_{coll}) in $p+p$ interactions at $\sqrt{s_{NN}}$=200 GeV. Nuclear modification factor R_{AA} [part (c)] and ratio R_2 (Part d) as a function of transverse momentum as predicted by HIJING v1.37 with (solid and dotted histogram) and without (dashed histogram) shadowing and quenching effects. The labels have the same meaning as in Fig. 4. The data are from PHENIX [10–12]. Only statistical error bars are shown.

To better understand why HIJING overpredicts the quenching of h^- for $p_T < 4$ GeV/c, we turn next to the latest data on identified π^0 central (0–10%) Au+Au collisions at $\sqrt{s_{NN}}$=200 GeV. We use these data because of much higher p_T reach than at $\sqrt{s_{NN}}$=130 GeV. Also in this case, Au+Au can be compared directly to the new $p+p$ data measured by PHENIX [11,12]. In Fig. 9(a), the predicted π^0 p_T spectra based on dE/dx=0, 0.5, and 2 GeV/fm are compared to the Au+Au data out to 8 GeV/c. In Fig. 9(b) the recent $p+p$ $\rightarrow \pi^0 + X$ data are compared to default HIJING. This shows even more clearly than the original test [37], how well HIJING is able to reproduce the high-p_T spectrum out to 10 GeV/c in the elementary $p+p$ case. The $R_{AA}(p_T)$ nuclear modification factor is shown in Fig. 9(c). It is observed that the default energy loss parameters dE/dx=2 GeV/fm describe very well the jet quenching pattern of neutral pions in central collisions. The Lund string fragmentation mechanism of hadronization in HIJING leads to a rather slow growth of R_{AA} to unity at high p_T [dashed histogram in Fig. 9(c)]. Only after $p_T > 4$ GeV/c do the details of hadronization become irrelevant, and in that range, the default energy loss leads to a factor of 5 suppression, in agreement with the naive surface emission estimate with λ=1 fm. The relative suppression ratio $R_2 \equiv R_{AA}(ysq)/R_{AA}(nsq)$ [Fig. 9(d)] shows in more detail the leveling off of R_2 beyond 4 GeV/c for the default energy loss, while it levels off at 0.4 for a reduced energy loss of 0.5 GeV/fm. Note that in all calculations the default p_0=2 GeV/c was used, as it has, however, no effect at high p_T.

In Fig. 10 we compare the quenching pattern of HIJING to data for peripheral (60–80%) reactions. Figure 10(b) is the pp data scaled by the number of collisions in this peripheral reaction class. The main difference with respect to Fig. 9 is that unlike in central collisions, even a reduced energy loss

dE/dx=0.5 GeV/fm overpredicts the small modification of R_{AA} from unity observed for more peripheral interactions. As more clearly seen in Fig. 10(d), HIJING predicts a 30% suppression in peripheral interactions that is not seen in the data. We conclude that while the central reaction suppression is correctly predicted by HIJING, the surface emission algorithm adopted to model energy loss is not realistic and does not reproduce the centrality dependence observed by PHENIX.

We have studied the dependence of the quenching pattern on variations of the mean free path parameter λ of HIJING as well. We find that the quenching is indeed sensitive to λ. In central collision increasing λ to 3 fm, for example, decreases the quenching for dE/dx=2 GeV/fm by a factor of approximately 2. To explain the centrality dependence an N_{part} dependence of λ must be assumed. We do not pursue here such an elaboration of the HIJING energy loss algorithm but future studies would be desirable to help distinguish between surface emission and volume emission models of jet energy loss.

The sensitivity of the nuclear modification factor $R_{AA}(p_\perp)$ to the mean energy loss parameter in HIJING at the lower 130A GeV energy is more clearly revealed in the high statistics computation shown in Fig. 11. The data at $\sqrt{s_{NN}}$=130 GeV are taken from PHENIX [6] and STAR [17]. This figure extends the comparison in Fig. 8 to the range p_T ~7 GeV/c. The main discrepancy between the negative hadrons h^- data and calculations is the observed distinct localized bump with a maximum at p_T~2 GeV/c. R_{AA} approaches the predicted quenching pattern with dE/dx=0.5 GeV/fm only at the highest p_T measured.

PHENIX has found that the excess negative hadrons in the 2–4 GeV range are, in fact, due to antiprotons [3]. In
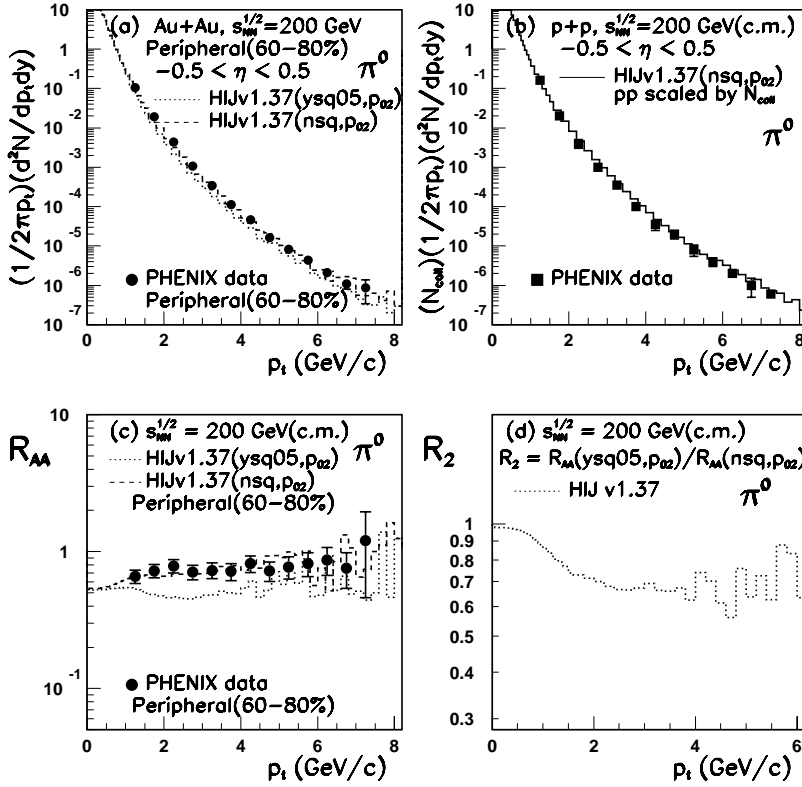
FIG. 10. Invariant yields at midrapidity for π^0 in central (60–80%) Au+Au collisions [Part (a)] and scaled by number of binary collisions (N_{coll}) in $p+p$ interactions at $\sqrt{s_{NN}}=200$ GeV. Nuclear modification factor R_{AA} [Part (c)] and ratio R_2 [Part (d)] as a function of transverse momentum as predicted by HIJING v1.37 with (solid histogram) and without (dashed histogram) shadowing and quenching effects. The labels have the same meaning as in Fig. 4. The data are from PHENIX [10–12]. Only statistical error bars are shown.
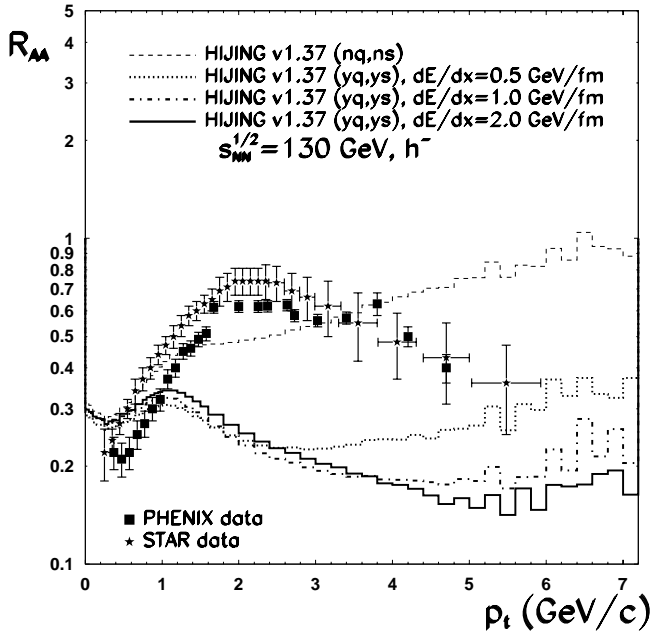

FIG. 11. Nuclear modification factor R_{AA}, as a function of transverse momentum as predicted by HIJING v1.37 for central (0–5%) Au+Au collisions at $\sqrt{s_{NN}}=130$ GeV. The different histograms are the results obtained without quenching and with quenching assuming different values for parton energy loss. The data are from PHENIX [6] (squares) and STAR [17] (stars). Only statistical error bars are shown.

order to check whether an enhanced baryon junction loop [86] mechanism could possibly account for that excess, we plot R_{AA} for HIJING/B$\overline{\text{B}}$ [87] in Fig. 12. While the junction source reduces the discrepancy between data and HIJING shown in Fig. 12(a), it fails to account for the very large excess of antiprotons at moderate p_T. From Figs. 12(a) and 12(b), we see that junctions as currently implemented do not solve the centrality dependence problem discussed in connection with Fig. 10 either.

As a final comment we compare the "central-to-peripheral" nuclear modification factor defined by

$$R_{AA}^{cp}(p_\perp) = \frac{(Yield/\langle N_{coll}\rangle)_{(0-5\%)}}{(Yield/\langle N_{coll}\rangle)_{(60-80\%)}}, \qquad (2)$$

where Yield$=(1/N_{events})(1/2\pi p_\perp)(d^2N/dp_\perp d\eta)$ to calculated values for this particular ratio. The data are from PHENIX [6,8] and STAR [17]. Even though B$\overline{\text{B}}$ version fails to describe both the numerator [Fig. 12(a)] and the denominator [Fig. 12(b)], it accidentally describes the R_{AA}^{cp} ratio of central collisions [Fig. 13(a)]. No such lucky coincidence occurs for peripheral collisions using the default HIJING [Fig. 13(b)]. This figure demonstrates the great care one must exercise in interpreting any agreement of dynamical models with specific ratios. It is always essential to check whether the model is able to reproduce the absolutely normalized spectra, as in Figs. 9 and 10. Only after a model passes that test can any agreement with specific data ratios be considered seriously.
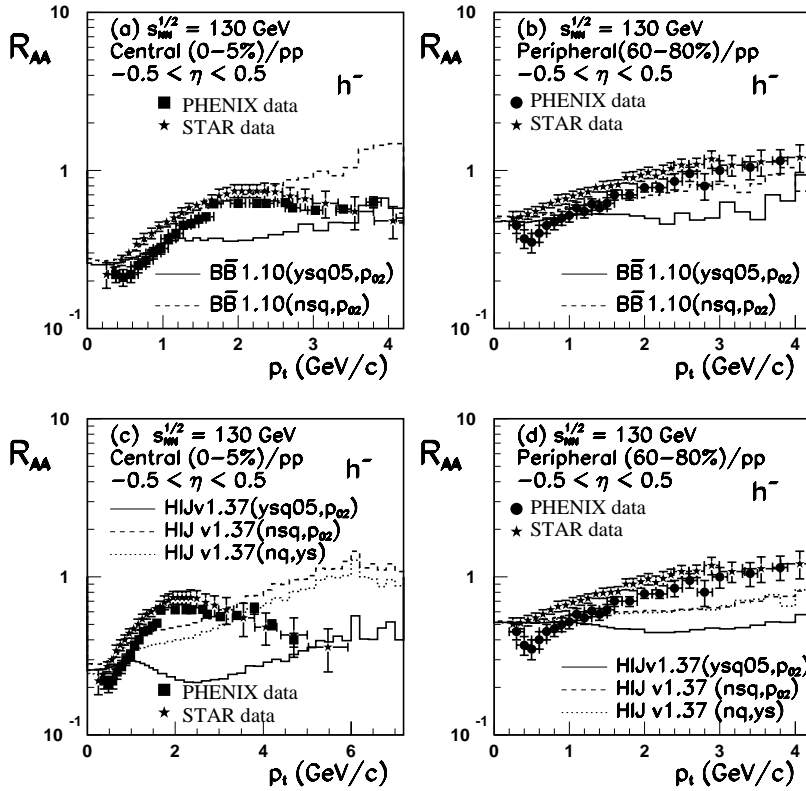
FIG. 12. Comparison of the nuclear modification factor $\bar{R}_{AA}$ for Au+Au as predicted by HIJING/B$\bar{\text{B}}$ v1.10 (upper part) and HIJING v1.37 (lower part) for central (0–5%) and peripheral (60–80%) Au+Au collisions. The data are from PHENIX [6,8] and STAR [17]. Only statistical error bars are shown.

IV. SUMMARY AND CONCLUSIONS

We have investigated in this paper how the predictions of HIJING and RQMD exclusive nuclear collision event generators compare to the new available data from RHIC. We concentrated on two classes of observables. First the global number and transverse energy distribution in rapidity was considered. Then we focused on the new jet quenching nuclear modification factors.

The energy dependence of global observables rule out RQMD because of its neglect of hard pQCD minijet production. However, the observed energy dependence also rules out HIJING in its default parameter settings. The separation scale p_0 between soft and hard processes, which assumed in HIJING to be a constant 2 GeV/c independent of $\sqrt{s}$ and centrality, predicts a too rapid growth of multiplicity. Motivated by FSS and ISS parton saturation models and the data, we tested and found that allowing a 10% growth of p_0 from 2.0 to 2.18 GeV greatly improved the consistency of HIJING

results with the observed RHIC systematics. In all cases, the default shadowing (with identical quark and gluon shadowing) assumed was found to be essential to reduce the minijet flux and not to over-predict the multiplicity. The small enhancement of the multiplicity due to jet quenching with the default energy loss was consistent with experimental data once the small energy dependence of p_0 is taken into account.

Our analysis of the jet quenching pattern predicted by HIJING shows that the default $dE/dx = 2$ GeV/fm accounts remarkably well for the suppression pattern of π^0 out to $p_T = 8$ GeV/c as observed for central Au+Au collisions at $\sqrt{s_{NN}} = 200$ GeV. A major advantage of HIJING over other models is that it reproduces accurately both the low-p_T dominated rapidity density and the high-p_T recent 200-GeV $p+p \rightarrow \pi^0 + X$ data [12] at the same time.

However, neither HIJING nor HIJING/B$\bar{\text{B}}$ are able to account for the anomalous baryon lump in the intermediate
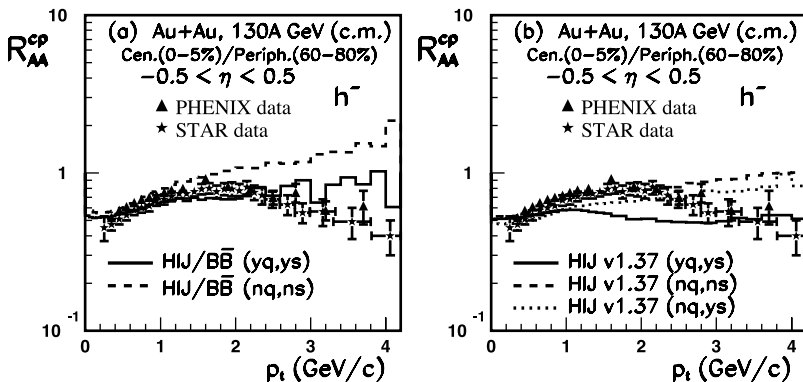

FIG. 13. Comparison of the nuclear modification factor $\bar{R}_{AA}^{cp}$ for Au+Au as predicted by HIJING/B$\bar{\text{B}}$ v1.10 [part (a)] and HIJING v1.37 [part (b)] for ratio of central (0–5%) to peripheral (60–80%) collisions. The data are from PHENIX [6,8] and STAR [17]. Only statistical error bars are shown.

$p_T < 4$ GeV/c region. Furthermore, we noted that the energy loss algorithm in HIJING corresponds effectively to surface emission with a default $\lambda = 1$ fm mean free path. We checked that increasing λ leads to less suppression. We found that a constant N_{part} independent λ, however, is not compatible with the observed centrality dependence of jet quenching.

The failure of the current implementation of baryon junction loops in HIJING/B$\bar{\text{B}}$ v1.10 to reproduce the observed p_T enhancement of antibaryons and baryons needs, however, further study since an enhancement was theoretically anticipated [89,86]. We are currently investigating why this feature of baryon junction dynamics did not emerge from numerical simulations with this code. Understanding the physical origin of the (anti) baryon anomalies is essential to disentangle competing mechanisms such as collective hydrodynamic flow [41], multi-quark coalescence [111], and possibly novel baryon junction dynamics [48] at RHIC.

ACKNOWLEDGMENTS

[1] *Proceedings of the 15th International Conference on Ultra-Relativistic Nucleus-Nucleus Collisions (QM01), Long Island, New York*, edited by T. J. Halman, D. E. Kharzeev, J. T. Mitchell, and T. Ullrich (BNL, Upton, N.Y., 2001) [Nucl. Phys. **A698**, 1 (2002)].

[2] *Proceedings of the 16th International Conference on Ultra-Relativistic Nucleus-Nucleus Collisions (QM02), Nantes, France*, edited by H. Gutbrod, J. Aichelin, and K. Werner [Nucl. Phys. **A715**, 1 (2003)].

[3] W. A. Zajc *et al.*, PHENIX Collaboration, Nucl. Phys. **A698**, 39c (2002).

[4] K. Adcox *et al.*, PHENIX Collaboration, Phys. Rev. Lett. **86**, 3500 (2001).

[5] K. Adcox *et al.*, PHENIX Collaboration, Phys. Rev. Lett. **87**, 052301 (2001).

[6] K. Adcox *et al.*, PHENIX Collaboration, Phys. Rev. Lett. **88**, 022301 (2002).

[7] K. Adcox *et al.*, PHENIX Collaboration, Phys. Rev. Lett. **89**, 212301 (2002).

[8] K. Adcox *et al.*, PHENIX Collaboration, Phys. Lett. B **561**, 82 (2003).

[9] A. Bazilevski *et al.*, PHENIX Collaboration, Nucl. Phys. **A715**, 486c (2003).

[10] J. Jia *et al.*, PHENIX Collaboration, Nucl. Phys. **A715**, 769c (2003).

[11] S. Adler *et al.*, PHENIX Collaboration, nucl-ex/0304022; S. Adler *et al.*, Phys. Rev. Lett. **91**, 072301 (2003).

[12] S. Adler *et al.*, PHENIX Collaboration, hep-ex/0304038; S. Adler *et al.*, Phys. Rev. Lett. (submitted).

[13] S. Adler *et al.*, PHENIX Collaboration, nucl-exp/0306021; S. Adler *et al.*, Phys. Rev. Lett. (submitted).

[14] J. Harris *et al.*, STAR Collaboration, Nucl. Phys. **A698**, 64c (2002).

[15] K. H. Ackermann *et al.*, STAR Collaboration, Phys. Rev. Lett. **86**, 402 (2001).

[16] C. Adler *et al.*, STAR Collaboration, Phys. Rev. Lett. **87**, 112303 (2001).

[17] C. Adler *et al.*, STAR Collaboration, Phys. Rev. Lett. **89**, 202301 (2002).

[18] J. C. Dunlop *et al.*, STAR Collaboration, Nucl. Phys. **A698**, 515c (2002).

[19] G. Kunde *et al.*, STAR Collaboration, Nucl. Phys. **A715**, 189c (2003).

[20] C. Adler *et al.*, STAR Collaboration, Phys. Rev. Lett. **90**, 082302 (2003).

[21] C. Adler *et al.*, STAR Collaboration, Phys. Rev. Lett. **90**, 032301 (2003).

[22] J. Adams *et al.*, STAR Collaboration, nucl-ex/0305015; J. Adams *et al.*, Phys. Rev. Lett. (submitted).

[23] J. Adams *et al.*, STAR Collaboration, nucl-ex/0306024; J. Adams *et al.*, Phys. Rev. Lett. **91**, 072304 (2003).

[24] G. Roland *et al.*, PHOBOS Collaboration, Nucl. Phys. **A698**, 54c (2002).

[25] B. B. Back *et al.*, PHOBOS Collaboration, Nucl. Phys. **A698**, 555c (2002).

[26] B. B. Back *et al.*, PHOBOS Collaboration, Phys. Rev. Lett. **85**, 3100 (2000).

[27] B. B. Back *et al.*, PHOBOS Collaboration, Phys. Rev. Lett. **87**, 102303 (2001).

[28] B. B. Back *et al.*, PHOBOS Collaboration, Phys. Rev. Lett. **88**, 022302 (2002).

[29] B. B. Back *et al.*, PHOBOS Collaboration, Phys. Rev. Lett. **89**, 222301 (2002).

[30] B. B. Back *et al.*, PHOBOS Collaboration, nucl-ex/0302015.

[31] B. B. Back *et al.*, PHOBOS Collaboration, nucl-ex/0306025; B. B. Back *et al.*, Phys. Rev. Lett. **91**, 072302 (2003).

[32] F. Viedebeck *et al.*, BRAHMS Collaboration, Nucl. Phys. **A698**, 29c (2002).

[33] I. G. Bearden *et al.*, BRAHMS Collaboration, Phys. Rev. Lett. **88**, 202301 (2002).

[34] D. Ouerdane *et al.*, BRAHMS Collaboration, Nucl. Phys. **A715**, 478 (2003).

[35] I. G. Bearden *et al.*, BRAHMS Collaboration, Phys. Rev. Lett. **90**, 102301 (2003).

[36] I. Arsene *et al.*, BRAHMS Collaboration, nucl-ex/0307003; I. Arsene *et al.*, Phys. Rev. Lett. **91**, 072305 (2003)

[37] X.-N. Wang and M. Gyulassy, Phys. Rev. D **44**, 3501 (1992); **45**, 844 (1992); M. Gyulassy and X.-N. Wang, Comput. Phys.

Commun. **83**, 307 (1994); X.-N. Wang, Phys. Rep. **280**, 287 (1997); Nucl. Phys. **A661**, 609c (1999).

[38] H. Sorge, Phys. Rev. C **52**, 3291 (1995); Z. Phys. C **67**, 479 (1995); M. Berenguer, H. Sorge, and W. Greiner, Phys. Lett. B **332**, 15 (1994).

[39] S. A. Bass *et al.*, Nucl. Phys. **A661**, 205c (1999), and reference therein.

[40] M. Gyulassy, I. Vitev, X.-N. Wang, and B.-W. Zhang, *Quark Gluon Plasma 3*, edited by R. C. Hwa and X.-N. Wang (World Scientific, Singapore, 2003), and reference therein.

[41] P. F. Kolb and U. Heinz, in *Quark Gluon Plasma 3* (Ref. [40]), and references therein.

[42] P. Braun-Munzinger, K. Redlich, and J. Stachel, in *Quark Gluon Plasma 3* (Ref. [40]), and references therein.

[43] E. Iancu and R. Vernugopalan, in *Quark Gluon Plasma 3* (Ref. [40]), and references therein.

[44] X.-N. Wang, Phys. Rev. C **61**, 064910 (2000).

[45] M. Gyulassy, I. Vitev, and X.-N. Wang, Phys. Rev. Lett. **86**, 2537 (2001).

[46] M. Gyulassy, P. Levai, and I. Vitev, Nucl. Phys. **B594**, 371 (2001); Phys. Rev. Lett. **85**, 5535 (2000); Nucl. Phys. **A661**, 637 (1999).

[47] M. Gyulassy, P. Levai, and I. Vitev, Phys. Lett. B **538**, 282 (2002).

[48] I. Vitev and M. Gyulassy, Phys. Rev. C **65**, 041902 (2002).

[49] M. Gyulassy, I. Vitev, X.-N. Wang, and P. Huovinen, Phys. Lett. B **526**, 301 (2002).

[50] I. Vitev and M. Gyulassy, Phys. Rev. Lett. **89**, 252301 (2002).

[51] I. Vitev, Phys. Lett. B **562**, 36 (2003).

[52] X.-N. Wang, Phys. Rev. C **63**, 054902 (2001).

[53] E. Wang and X.-N. Wang, Phys. Rev. C **64**, 034901 (2001).

[54] S. Y. Li and X.-N. Wang, Phys. Lett. B **527**, 85 (2002).

[55] E. Wang and X.-N. Wang, Phys. Rev. Lett. **89**, 162301 (2002).

[56] P. Levai, G. Papp, G. G. Barnafoldi, and G. Fai, nucl-th/0306019.

[57] K. J. Eskola, K. Kajnatie, P. V. Ruuskanen, and K. Tuominen, Phys. Lett. B **543**, 208 (2002); **497**, 39 (2001); Nucl. Phys. **B570**, 379 (2000).

[58] K. J. Eskola, Nucl. Phys. **A698**, 78c (2002).

[59] D. Kharzeev and M. Nardi, Phys. Lett. B **507**, 121 (2001).

[60] D. Kharzeev and E. Levin, Phys. Lett. B **523**, 79 (2001).

[61] D. Kharzeev, E. Levin, and K. Tuchin, Phys. Lett. B **547**, 21 (2002).

[62] J. Schaffner-Bielich, D. Kharzeev, L. McLerran, and R. Vernugopalan, Nucl. Phys. **A705**, 494 (2002).

[63] D. Kharzeev, E. Levin, and L. McLerran, Phys. Lett. B **561**, 93 (2003).

[64] W. Cassing and E. L. Bratkovskaya, Phys. Rep. **308**, 65 (1999); W. Cassing, E. L. Bratkovskaya, and S. Juchem, Nucl. Phys. **A674**, 249 (2000).

[65] Z. W. Lin, S. Pal, C. M. Ko, Bao-An Li, and Bin Zhang, Phys. Rev. C **64**, 011902 (2001).

[66] Z. W. Lin and C. M. Ko, Phys. Rev. C **65**, 034904 (2002).

[67] Z. W. Lin, C. M. Ko, and S. Pal, Phys. Rev. Lett. **89**, 152301 (2002).

[68] Z. W. Lin, S. Pal, C. M. Ko, B. A. Li, and B. Zhang, Nucl. Phys. **698**, 375 (2002).

[69] D. Molnar and M. Gyulassy, Nucl. Phys. **A697**, 495 (2002); **A703**, 893(E) (2002).

[70] D. Molnar and M. Gyulassy, nucl-th/0211017.

[71] S. A. Bass *et al.*, Prog. Part. Nucl. Phys. **41**, 225 (1998).

[72] M. J. Bleicher, S. A. Bass, L. V. Bravina, W. Greiner, S. Soff, H. Stöcker, N. Xu, and E. E. Zabrodin, Phys. Rev. C **62**, 024904 (2000).

[73] N. Armesto and C. Pajares, Int. J. Mod. Phys. A **15**, 2019 (2000).

[74] A. Capella and D. Sousa, Phys. Lett. B **511**, 185 (2001).

[75] S. Jeon and J. Kapusta, Phys. Rev. C **63**, 011901 (2001).

[76] D. E. Kahana and S. H. Kahana, Phys. Rev. C **63**, 031901 (2001).

[77] L. McLerran and R. Venugopalan, Phys. Rev. D **49**, 2233 (1994); **50**, 2225 (1994).

[78] Yu. V. Kovchegov, Phys. Rev. D **54**, 5463 (1996).

[79] M. Gyulassy and M. Plumer, Phys. Lett. B **243**, 432 (1990).

[80] M. M. Aggarwal *et al.*, WA98 Collaboration, Eur. Phys. J. C **23**, 225 (2002).

[81] X.-N. Wang and M. Gyulassy, Phys. Rev. Lett. **68**, 1480 (1992).

[82] R. Baier, Y. L. Dokshitzer, S. Peigne, and D. Schiff, Phys. Lett. B **345**, 277 (1995); Phys. Rev. C **58**, 1706 (1998); R. Baier, D. Schiff, and B. G. Zakharov, Annu. Rev. Nucl. Part. Sci. **50**, 37 (2000); R. Baier, Y. L. Dokshitzer, A. H. Muller, and D. Schiff, J. High Energy Phys. **0109**, 033 (2001).

[83] M. Gyulassy and P. Levai, Phys. Lett. B **442**, 1 (1998).

[84] X.-N. Wang, Phys. Rev. Lett. **81**, 2655 (1998).

[85] S. E. Vance, M. Gyulassy, and X.-N. Wang, Phys. Lett. B **443**, 45 (1998).

[86] S. E. Vance and M. Gyulassy, Phys. Rev. Lett. **83**, 1735 (1999).

[87] See http://www-cunuke.phys.columbia.edu/people/svance/hijbb.html; S. E. Vance, Ph.D. thesis, Columbia University, 1999.

[88] G. C. Rossi and G. Veneziano, Nucl. Phys. **B123**, 507 (1977); Phys. Rep. **63**, 153 (1980).

[89] D. Kharzeev, Phys. Lett. B **378**, 238 (1996).

[90] L. D. Landau, Izv. Akad. Nauk SSSR, Ser. Fiz. **17**, 51 (1953).

[91] J. D. Bjorken, Phys. Rev. D **27**, 140 (1983).

[92] H. Stocker and W. Greiner, Phys. Rep. **137**, 277 (1986).

[93] P. F. Kolb, P. Huovinen, U. W. Heinz, and H. Heiselberg, Phys. Lett. B **500**, 232 (2001).

[94] P. Huovinen, P. F. Kolb, U. W. Heinz, P. V. Ruuskanen, and S. A. Voloshin, Phys. Lett. B **503**, 58 (2001).

[95] D. Teaney, J. Lauret, and E. V. Shuryak, nucl-th/0110037.

[96] P. Huovinen, nucl-th/0305064.

[97] T. Hirano and Y. Nara, nucl-th/0307015.

[98] F. Cooper and G. Frye, Phys. Rev. D **10**, 186 (1974).

[99] X.-N. Wang and M. Gyulassy, Phys. Rev. Lett. **86**, 3496 (2001).

[100] M. Gyulassy, Lect. Notes Phys. **37**, 1 (2002).

[101] G. J. Alner *et al.*, UA5 Collaboration, Z. Phys. C **33**, 1 (1986).

[102] W. Thome *et al.*, Aachen-CERN-Heidelberg-Munich Collaboration, Nucl. Phys. **B129**, 365 (1977).

[103] J. Whitmore, Phys. Rep. **10**, 273 (1974).

[104] C. Albajar *et al.*, Nucl. Phys. **B335**, 261 (1990).

[105] A. Dress, Nucl. Phys. **A698**, 331c (2002).

[106] A. Dress, in *Proceedings of the 30th International Workshop on Gross Proprieties on Nuclei and Nuclear Excitation, Hir-*

scheg, 2002, edited by M. Buballa, W. Norenberg, B.-J. Schaefer, and J. Wambach (GSI, Darmstadt, Germany, 2002), pp. 280–291.

[107] D. Kharzeev, E. Levin, and L. McLerran, Phys. Lett. B **561**, 93 (2003).

[108] E. Shuryak, Nucl. Phys. **A717**, 291 (2003); E. V. Shuryak and I. Zahed, Phys. Rev. D **67**, 054025 (2003).

[109] B. Muller, Phys. Rev. C **67**, 061901 (2003).

[110] K. Gallmeister, C. Greiner, and Z. Xu, Phys. Rev. C **67**, 044905 (2003).

[111] Z. W. Lin and C. M. Ko, Phys. Rev. Lett. **89**, 202302 (2002); D. Molnar and S. A. Voloshin, *ibid.* **91**, 092301 (2003); R. J. Fries, B. Muller, C. Nonaka, and S. Bass, *ibid.* **90**, 202303 (2003); nucl-th/0306027; R. C. Hwa and C. B. Yang, Phys. Rev. C **67**, 034902 (2003); V. Greco, C. M. Ko, and P. Levai, Phys. Rev. Lett. **90**, 202302 (2003).